Available online at www.sciencedirect.com
ScienceDirect
Journal of Nuclear Materials 367–370 (2007) 581–586
journal of nuclear materials
www.elsevier.com/locate/jnucmat

Fracture toughness properties in the transition region of the Eurofer97 tempered martensitic steel

R. Bonadé, P. Spätig *, N. Baluc

Fusion Technology-Materials, CRPP EPFL, Association EURATOM-Confédération Suisse, 5232 Villigen PSI, Switzerland

Abstract

A fracture toughness database obtained on the Eurofer97 steel (25 mm plate, heat 83697) is presented. The material has been tested in the 'as-received' condition in the lower transition region at temperatures ranging from 173 K down to 123 K. Sub-sized (0.35T) compact tension specimens, 0.35T C(T), have been used in this study. The database is analyzed in the framework of ASTM E-1921–03 standard. The results indicate that the median toughness–temperature curve of the Eurofer97 is steeper than the master curve for 'ferritic' steels used in the ASTM E-1921 framework. This database is also compared with fracture toughness data obtained on different Eurofer97 heats and previously reported in the literature. Modest variations in the reference temperature T_0 used to index the fracture toughness–temperature curve were found between the different heats.

1. Introduction

The ASTM-E-1921 Master Curve Standard [1] has been developed to index the median toughness–temperature curve, $K_{med}(T)$, on an absolute temperature scale at a median reference toughness level. One of the underlying assumptions of the master-curve is that there is a universal shape of the $K_{med}(T)$ curve for 'ferritic' steels. The master-curve expression has been derived from the analysis of large experimental fracture databases of reactor pressure vessel (RPV) steels in the transition region [2]. It has been recently shown by Odette et al. [3] that it is possible to apply the master-curve concept to steels other than the RPV steels, such as tempered-martensitic steels. In this sense, the fracture toughness database generated for the F82H-mod steel has been successfully described in terms of the ASTM E-1921 standard.

In order to characterize the fracture properties in the lower transition region of the 9CrWVTa Eurofer97 steel (25 mm plate, heat 83697), we have generated an extensive fracture database with compact tension C(T) specimens. The experimental results presented have been extracted from a more extensive work aimed at studying and at modeling the fracture properties of the Eurofer97 in the ductile-to-brittle transition region. Due to limitations on space, we only present here the database for 0.35T C(T) specimens, together with relevant results related to the applicability of the master-curve concept to the Eurofer97 steel. The complete Eurofer97

* Corresponding author. Tel.: +41 56 310 29 34; fax: +41 56 310 45 29.
E-mail address: philippe.spatig@psi.ch (P. Spätig).

0022-3115/$ - see front matter © 2007 Elsevier B.V. All rights reserved.
doi:10.1016/j.jnucmat.2007.03.031

database including 0.2T C(T) results can be found in [4].

2. Experimental procedures

The fracture toughness data have been obtained by testing 0.35T C(T) specimens cut from a 25 mm thick Eurofer97 plate (Heat 83697). The specimens have been tested at five different temperatures: 173 K (33 specimens), 153 K (27 specimens), 144 K (15 specimens), 135 K (12 specimens) and 125 K (5 specimens), using a constant machine cross-head velocity of 0.1 mm/min. Most of the tests have been performed in the L–T orientation (see Table 1). A temperature chamber equipped with a PID controller allowed reaching a temperature stability of ±1 K during the tests. In all the cases, the specimen temperature was measured by a thermocouple (K-type) directly attached to its surface near the crack tip.

The results of the fracture toughness tests have been evaluated in terms of the elastic–plastic K_{J_c} parameter, which is derived from the value of the J-integral at the onset of cleavage fracture, J_C [1].

3. Results and discussion

The results obtained are summarized in Table 1 and are plotted in Fig. 1 and show the temperature dependence of fracture toughness in the lower transition region without any type of correction (neither statistical nor constraint loss). Two K_{J_c} limits associated with two constraint levels as defined by the M factor [5] are also indicated (for $M = 30$ and $M = 70$):

$$M = \frac{Eb_0\sigma_{0.2}}{(1-\nu^2)K_{J_c}^2}, \tag{1}$$

where E is Young's modulus, b_0 is the ligament length, $\sigma_{0.2}$ is the yield stress, ν is the Poisson's coefficient. Since fracture toughness is also related to the critical crack tip opening, δ_c, through the following equation [6]:

$$J_c = K_{J_c}^2\frac{(1-\nu^2)}{E} = m\delta_c, \tag{2}$$

where m is a factor depending on the specimen geometry and the material properties, M can also be written as:

$$M = \frac{b_0}{m\delta_c}. \tag{3}$$

Thus the M factor scales with the inverse of the crack tip opening. As it can be observed in Fig. 1, the lowest constraint level, as reflected by the lowest M value corresponding to the highest fracture toughness value at $T = 173$ K, is about 70. All these presented data are therefore significantly more constrained than the K_{J_c} limit associated with $M = 30$ as request by the ASTM E1921.

The dataset at 173 K has been analyzed following the ASTM E-1921–03 procedure to determine the reference temperature T_0. In order to do so, first the raw data were statically adjusted to the 1 T standard crack front dimension according to:

$$K_{1T} = 20 + [K_{0.35T} - 20]\cdot\left(\frac{B_{0.35T}}{B_{1T}}\right)^{1/4}. \tag{4}$$

We obtained a value of $T_0 = 184$ K. The ASTM E-1921 master-curve is plotted in Fig. 2 together with the experimental dataset. The upper and lower bounds representing the 99% and 1% failure probabilities respectively are also shown in the plot. The analysis of Fig. 2 suggests that the master-curve expression given by the standard does not describe satisfactorily the evolution of $K_{J_c}(\mathrm{med})$ with temperature. A multi-temperature analysis of the data including both the 173 K and the 153 K datasets does not improve the description of the experimental results. In fact, the experimental data clearly show that $K_{J_c}(\mathrm{med})$ increases faster with T than the prediction of the ASTM E-1921 master-curve. Based on the statistical analysis of the experimental data, we have determined a new expression for the evolution of $K_{J_c}(\mathrm{med})(T)$. In fact, we adjusted the steepness of the transition by fitting the exponential parameter, finding that the following expression provides a better description of $K_{\mathrm{med}}(T)$:

$$K_{\mathrm{med}} = 30 + 70\exp(0.04(T - T_0)) \tag{5}$$

We have calculated T_0 using now Eq. (5) instead of the standard master-curve expression, and obtained $T_0 = 179$ K. The results are presented in Fig. 3. As it can be observed, the statistical description of the experimental dataset is very good. Some additional C(T) data obtained by Rensman [7] for the 25 mm thick Eurofer97 plate are also included for comparison; both datasets are observed to be in good agreement with each other. For the time being, the physical origin of the difference in the $K_{J_c}(\mathrm{med})(T)$ shape between Eurofer97 and F82H is not well understood. Nonetheless, it is believed that the content and size distribution of inclusions and/or carbides (regarded as potential fracture initiators)

Table 1
Fracture toughness data, Eurofer97 – heat 83697

Specimen ID	a_0/W	P_f (N)	K_{Jc} (MPa · $m^{1/2}$)		M	Orientation
			0.35T C(T)	Adjusted to 1T		
Test temperature: 125 K $\sigma_{0.2}$ = 885 MPa – E = 217.1 GPa			*Specimen type: 0.35T C(T) Dimensions: B = 9 mm, W = 18 mm*			
A5	0.55	4946	45.6	39.7	841.0	L–T
A4	0.53	4880	42.3	37.2	1021.9	L–T
A3	0.54	4757	43.0	37.8	964.2	L–T
A2	0.54	3850	34.7	31.3	1482.7	L–T
A1	0.54	4517	40.2	35.6	1105.3	L–T
Test temperature: 135 K $\sigma_{0.2}$ = 826 MPa – E = 216.6 GPa			*Specimen type: 0.35T C(T) Dimensions: B = 9 mm, W = 18 mm*			
B30	0.49	7457	57.1	48.6	565.3	L–T
B27	0.50	5354	42.1	37.1	1019.0	L–T
B24	0.51	5452	44.2	38.6	908.5	L–T
B23	0.48	4956	37.3	33.3	1353.6	L–T
B22	0.49	6515	49.6	42.9	748.0	L–T
B20	0.47	6711	49.4	42.7	784.9	L–T
B11	0.47	6721	49.2	42.6	790.3	L–T
A27	0.50	4342	32.5	29.6	1711.8	L–T
A12	0.50	5422	39.3	34.9	1171.7	L–T
A11	0.47	6426	46.9	40.8	870.1	L–T
A10	0.50	5840	43.1	37.8	974.6	L–T
A8	0.47	5365	39.4	35.0	1232.6	L–T
Test temperature: 144 K $\sigma_{0.2}$ = 727 MPa – E = 216.1 GPa			*Specimen type: 0.35T C(T) Dimensions: B = 9 mm, W = 18 mm*			
B29	0.46	6117	43.5	38.1	907.3	L–T
B26	0.47	5685	40.8	36.0	1011.4	L–T
B25	0.47	6900	49.8	43.0	677.9	L–T
B21	0.53	6925	49.0	42.4	620.2	L–T
B19	0.48	7643	57.7	49.0	496.5	L–T
B18	0.49	6730	51.4	44.3	611.7	L–T
B17	0.48	6679	49.6	42.8	671.6	L–T
B16	0.49	7082	54.1	46.3	552.4	L–T
B15	0.47	8867	65.0	54.7	398.6	L–T
B14	0.48	6567	49.3	42.6	679.2	L–T
B13	0.48	7021	52.4	45.0	601.9	L–T
B10	0.49	5282	40.6	35.9	983.3	L–T
B9	0.48	8453	63.3	53.4	412.5	L–T
B8	0.48	8696	65.7	55.3	382.3	L–T
B7	0.49	7869	60.2	51.0	447.3	L–T
Test temperature: 153 K $\sigma_{0.2}$ = 697 MPa – E = 215.6 GPa			*Specimen type: 0.35T C(T) Dimensions: B = 9 mm, W = 18 mm*			
B6	0.47	9278	66.7	56.0	343.9	L–T
B5	0.49	8272	62.9	53.1	372.2	L–T
B4	0.50	7681	55.2	47.2	473.7	L–T
B2	0.48	7560	56.3	48.0	473.6	L–T
B1	0.48	8213	61.2	51.8	400.8	L–T
A30	0.46	6642	46.7	40.6	714.8	L–T
A29	0.47	6796	48.8	42.2	642.5	L–T
A25	0.47	9391	69.1	57.9	320.5	L–T
A24	0.47	5297	38.1	34.0	1054.1	L–T
A19	0.49	8511	64.7	54.5	351.7	L–T
A18	0.47	5628	40.5	35.8	932.9	L–T
A17	0.45	10249	70.8	59.2	316.8	L–T
A16	0.46	8884	62.7	52.9	396.6	L–T
A15	0.47	8520	61.1	51.7	409.9	L–T
A14	0.46	7568	53.1	45.5	552.9	L–T
A13	0.47	9055	64.9	54.6	363.3	L–T
B3	0.47	9252	66.9	56.2	341.9	L–T
B28	0.48	10385	77.7	64.5	248.7	L–T

(*continued on next page*)

Table 1 (*continued*)

Specimen ID	a_0/W	P_f (*N*)	K_{Jc} (MPa · m$^{1/2}$)		*M*	Orientation
			0.35T C(T)	Adjusted to 1T		
A9	0.48	11356	85.0	70.1	207.8	L–T
A8-2	0.49	9219	71.3	59.6	289.6	T–L
A8-1	0.48	10982	81.9	67.8	223.8	T–L
A7-2	0.48	7032	53.1	45.5	532.4	T–L
A7-1	0.46	10548	74.4	62.0	281.6	T–L
A6-2	0.49	10895	83.0	68.6	213.7	T–L
A6-1	0.47	7891	57.2	48.7	467.7	T–L
A5-2	0.47	6058	43.5	38.1	808.6	T–L
A5-1	0.50	5641	44.4	38.8	732.2	T–L
Test temperature: 173 K $\sigma_{0.2}$ = 666 MPa – E = 214.6 GPa			*Specimen type: 0.35T C(T) Dimensions: B = 9 mm, W = 18 mm*			
A21	0.47	11625	109.51	89.1	127.6	L–T
A22	0.48	13822	139.33	112.1	77.3	L–T
A26	0.48	13930	141.18	113.5	75.3	L–T
A28	0.50	8215	69.9	58.5	295.4	L–T
B11	0.50	12587	165.9	132.6	52.4	L–T
B1.1	0.50	7138	57.10	48.6	442.7	L–T
B1.2	0.50	12080	138.0	111.0	75.8	L–T
B2.1	0.50	11964	121.7	98.5	97.5	L–T
B2.2	0.50	10614	107.34	87.4	125.3	L–T
B3.1	0.50	12220	137.71	110.8	76.1	L–T
B3.2	0.50	8601	76.16	63.3	248.9	L–T
B4.1	0.50	10813	107.89	87.8	124.0	L–T
B4.2	0.49	10817	104.6	85.3	134.6	L–T
B5.1	0.50	8558	74.56	62.1	259.7	L–T
B5.2	0.49	8312	72.00	60.1	284.0	L–T
B6.1	0.50	10530	104.26	85.0	132.8	L–T
B6.2	0.50	10582	108.9	88.6	121.7	L–T
B7.1	0.50	12395	142.27	114.3	71.3	L–T
B7.2	0.49	8182	69.70	58.3	303.1	L–T
B8.1	0.48	11841	124.87	100.9	96.3	L–T
B8.2	0.50	10129	96.62	79.1	154.6	L–T
B9.1	0.50	11504	115.47	93.7	108.3	L–T
B9.2	0.50	9460	91.71	75.3	171.6	L–T
B10.2	0.50	9280	90.52	74.4	176.2	L–T
B11.1	0.50	9685	93.91	77.0	163.7	L–T
B12.1	0.50	10602	102.76	83.9	136.7	L–T
B12.2	0.48	12277	119.36	96.7	105.4	L–T
B13.1	0.50	8788	78.26	64.9	235.7	L–T
B13.2	0.49	10579	98.25	80.4	152.5	L–T
B14.1	0.50	9227	83.17	68.7	208.7	L–T
B14.2	0.49	10932	105.33	85.8	132.7	L–T
B15.1	0.49	11453	106.50	86.7	129.8	L–T
B15.2	0.49	11117	112.49	91.4	116.4	L–T

between the two steels are different enough to lead to the observed difference of the $K_{J_c}(\mathrm{med})(T)$ shape. A detailed comparative microstructural study has been initiated and is currently in progress to address this issue.

Rensman has also presented a fracture database for the Eurofer97, 8 mm and 14 mm plates [7]. For the sake of comparison, we have only considered C(T) data, which have been analyzed by using the ASTM E 1921 standard, substituting the master-curve expression by Eq. (5). The reference temperature T_0 for these plates was determined using the multi-temperature approach and a value equal to 161 K was found. The two thin plates (8 mm and 14 mm) appear then tougher than the 25 mm thick. The data for the 8 mm and 14 mm plates are plotted in Fig. 4 together with the datasets presented previously for the 25 mm plate. The description of the experimental data as given by Eq. (5) is excellent. Note that the curve representing the 1% cumulative probability to fracture perfectly bounds the dataset, offering a conservative description for the risk of

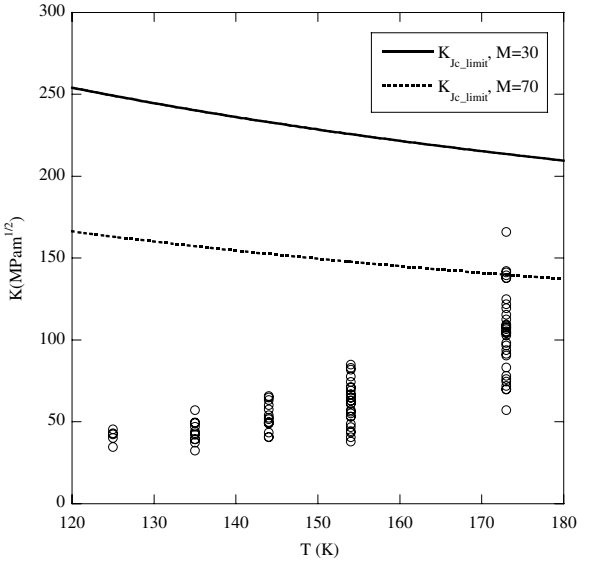

Fig. 1. Fracture toughness data versus temperature obtained with 0.35T C(T) specimens. K_{Jc} limit associated with $M = 70$ and $M = 70$.

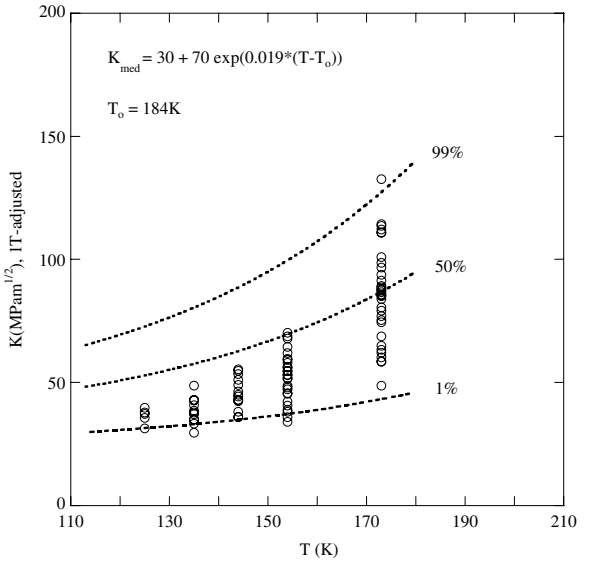

Fig. 2. Predictions of the ASTM E1921 standard for the Eurofer97. T_0 has been calculated by considering only the data at 173 K.

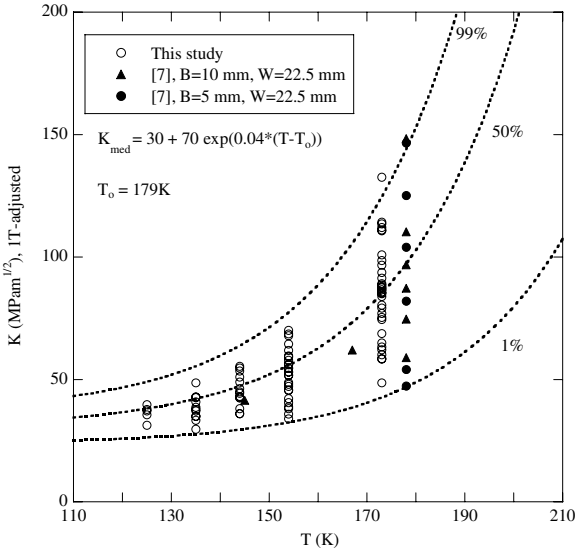

Fig. 3. Evolution of the fracture toughness with temperature as described by Eq. (5). C(T) data.

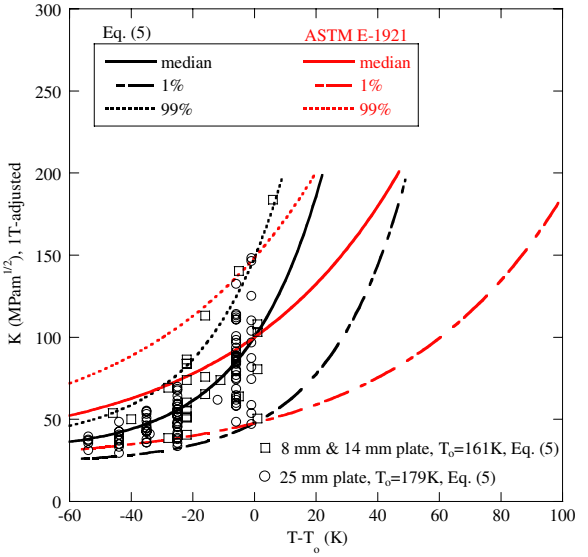

Fig. 4. Compilation of the available fracture toughness data for Eurofer97 (8, 14 and 25 mm plates). C(T) data.

catastrophic failure. From an integrity assessment point of view, the validation of Eq. (5) as a proper description for the evolution of K_{j_c}(med) with T is a critical issue. When the lower bound (1% failure probability for instance) is considered to represent the loading limit for the safe operation conditions of a structure, the operational temperature range associated with Eq. (5) is more extended in the low temperature range than that determined with the ASTM E1921 master-curve.

4. Conclusions

A reference fracture toughness-temperature curve for the Eurofer97 tempered martensitic steel was established in the low transition region by

testing 0.35T C(T) specimens. A large number of tests have been performed at five temperatures. The scatter exhibited by the fracture toughness values in the transition region and its evolution with temperature were successfully accounted for by modifying the shape of the ASTM E-1921 master-curve. In this sense, the 99% upper and 1% lower failure probability limits were observed to bound correctly the experimental data. The experimental results indicate that the shape of the Eurofer97 $K_{J_c}(\mathrm{med})(T)$ curve is steeper than that of the RPV steel as described by the ASTM E-1921 standard. All the specimens were tested at temperatures for which the M value, characterizing the constraint level was larger than 70, which is believed to be larger enough to avoid constraint loss on C(T) specimens.

The analysis of our results with other published data has revealed differences in fracture toughness between the different plates of Eurofer97, differences reflected in variation of about 20 K in the T_0 values.

Acknowledgements

The financial support of the Swiss National Foundation and of EURATOM is gratefully acknowledged. The Paul Scherrer Institute is acknowledged for providing access to its facility.

References

[1] Standard Test Method for Determination of Reference Temperature, T_0, for Ferritic Steels in the Transition Range, Annual Book of ASTM Standards 2004, Vol. 03.01, ASTM International, 2004.
[2] K. Wallin, Int. J. Pres. Ves. Pip 55 (1) (1993) 61.
[3] G.R. Odette, T. Yamamoto, H. Kishimoto, M. Sokolov, P. Spätig, W.J. Yang, J.W. Rensman, G.E. Lucas, J. Nucl. Mater. 329–333 (2004) 1243.
[4] R. Bonadé, PhD Thesis No. 3405, EPFL, Lausanne 2006.
[5] J.A. Joyce, R.L. Tregoning, Eng. Fract. Mech. 72 (2005) 1559.
[6] T.L. Anderson, Fracture Mechanics Fundamentals and Applications, 3rd Ed., CRC Press, 1995.
[7] J. Rensman, NRG-Report 20023/05.68497/P (2005).